Domain growth in the presence of quenched disorder

Arthur E. Bailey,[1,*] B. J. Frisken,[2] and David S. Cannell[3]
[1]*Exxon Research and Engineering, Annandale, New Jersey 08801*
[2]*Department of Physics, Simon Fraser University, Burnaby, British Columbia, Canada V5A 1S6*
[3]*Department of Physics, University of California at Santa Barbara, Santa Barbara, California 93106*
(Received 11 March 1997)

We describe the results of experiments investigating the growth dynamics of domains which form spontaneously in a portion of the one-phase region of a binary fluid mixture in the presence of quenched disorder. Dilute silica gels imbibed with mixtures of isobutyric acid and water were pressure quenched from an equilibrium one-phase state to a region of the phase diagram lying within the coexistence curve of the pure, or gel-free, system, but outside the coexistence curve of the gel-mixture system. Small-angle light-scattering measurements revealed a ring of scattered light which appeared at large scattering wave vectors and evolved to smaller scattering wave vectors in a manner consistent with $t^{1/3}$ domain growth; no evidence of domain pinning was observed during the first 1000 s following a quench. Furthermore, most measurements were consistent with dynamic scaling behavior. An unexpected feature of this system was the rapid growth of long-wavelength fluctuations immediately following the quench. [S1063-651X(97)10708-5]

PACS number(s): 64.70.Ja, 64.60.Ht, 68.45.Gd

I. INTRODUCTION

It is by now well established that three-dimensional random-field Ising magnets, when realized by subjecting an antiferromagnet diluted with impurities to a uniform magnetic field, enter a nonequilibrium domain state upon being cooled in the presence of the random field [1]. A sample subjected to such a field-cooling procedure falls out of equilibrium above the transition temperature at which long-range order develops in equilibrium. The origin of this behavior is believed to be the preference of spin fluctuations for regions in which, due to statistical fluctuations, the random field favors a particular spin orientation [2]. Energy barriers resulting from domain-wall pinning by the impurity atoms are then predicted to cause exponentially long relaxation times of this metastable domain state.

Another class of systems for which quenched, i.e., spatially fixed, impurities have major effects is that of fluids or binary fluid mixtures confined in porous media. In fact, inspired by work on magnetic systems and by early work on fluid mixtures in various gels [3], Brochard and de Gennes [4] suggested that the random-field Ising model might also apply to these systems. A particularly interesting medium is a dilute rigid network, as is found in some silica gels. The silica attracts the fluid phase, or preferentially attracts one of the two species of a binary mixture; thus it may be thought of as exerting a spatially localized field. Because the silica concentration is not uniform, even on long length scales, this field consists of both an average component and a spatially fluctuating component. These fluctuations are correlated over a distance which is determined by how the gel is made, and can be varied from below 100 Å up to thousands of Å.

To date, the equilibrium phase behavior of three gel-fluid systems has been investigated. Measurements of two gel-pure fluid systems (helium in aerogel [5] and nitrogen in aerogel [6]) and in one gel-binary mixture system [isobutyric acid–water (IBAW) in silica gel [7]] have revealed similar behavior. In all three cases, the coexistence curve of the gel-fluid system is drastically narrowed, is shifted to one side of the critical density or concentration of the pure, i.e., gel-free, system, and lies significantly below the coexistence curve of the corresponding pure system. The coexistence curve in both gel-pure fluid systems lies on the high-density side of the pure fluid's coexistence curve, and the coexistence curve of the gel-mixture system lies on the water-rich side of the pure mixture's coexistence curve. This behavior is consistent: the gels attract the fluid phases of helium and nitrogen, and preferentially attract water over IBA.

In light of the recent measurement of the equilibrium phase behavior of the IBAW-gel system, some of the effects observed in previous studies [8] of the same system are rather surprising. In particular, IBAW-gel samples, sufficiently rich in water, give every indication of phase separating when cooled into the vicinity of the coexistence curve of the pure IBA and water mixture. Each sample has a sharply defined temperature T^*, such that when cooled below T^* the scattered intensity both increases suddenly and dramatically, and develops a very slow (~ 10 s) dynamic time scale. Samples held below T^* for any appreciable time tend to become opaque and reequilibrate slowly after being heated above T^*. These observations are consistent with domain formation and growth. The long reequilibration time indicates that concentration differences are established on long length scales while the sample is held below T^*. Surprisingly, this behavior occurs in what is now known to be the *one*-phase region of the IBAW-gel system's phase diagram [7]. This behavior is strongly reminiscent of that observed for random-field magnets which enter a metastable domain state *above* the temperature at which long-range order develops.

Motivated by this similarity, we have studied the dynamics of the process whereby the IBAW-gel system enters its

*Present address: Scitech Instruments, North Vancouver, BC, Canada V7J 2S5.

version of the ''frozen-domain'' state. Small-angle light-scattering measurements were performed while rapidly pressure quenching samples from the stable one-phase state into the region of the phase diagram where the domains form. We observed scattering similar in many ways to that which is seen after similarly quenching a pure binary mixture into its two-phase region [9–11]: a ring of scattered light formed and grew rapidly in intensity while collapsing toward small angles. Somewhat surprisingly this process occurred on time scales quite similar to or even somewhat faster than those measured previously for pure IBAW mixtures [12], and continued until the ring of scattered light had collapsed below the smallest accessible scattering wave vector k (1722 cm^{-1}). This indicates that domains form and grow until they reach sizes of at least 10 μm, much larger than the correlation length of the gel, without showing any detectable sign of pinning or slow dynamics. Nevertheless, pinning must ultimately occur because samples left in the domain state have been observed to remain opaque for weeks [8], indicating that domain coarsening can eventually become very slow or stop altogether. In addition to the growth and collapse of a peak in the scattering, as is normally observed for a pure system undergoing phase separation, we also observed an effect not seen in pure mixtures: a strong simultaneous growth in the scattering at even the lowest k values accessible. This effect is not observed in either spinodal decomposition or nucleation for the pure mixture, but has been previously noted by Lee in a two-dimensional numerical simulation of spinodal decomposition in the presence of fixed impurities [13].

II. EXPERIMENT

A. Sample preparation and gel properties

The rigid silica gels used in these studies all contained 4% silica by weight (wt %). The gels were prepared from solutions of tetramethylorthosilicate or TMOS ($\mathrm{Si[OCH_3]_4}$) in water using a two-step process [14]. They were grown in stainless-steel scattering cells containing two 0.25-mm-thick flexible glass windows clamped 2.0 mm apart, with a clear diameter of 2.0 cm. The solutions gelled at room temperature, and were aged for a time roughly equal to ten times the gelation time. The gels were never dried.

These gels are easily characterized by scattering. They scatter isotropically on length scales larger than a gel correlation length ξ_G ($k<\xi_G^{-1}$), and like mass fractals with fractal dimension D_f at small length scales ($k>\xi_G^{-1}$) [15]. Thus the structure of the gels is consistent with deviations in local silica concentration correlated up to distances of order ξ_G. These correlations fall off rapidly for length scales $\geqslant\xi_G$. Fluctuations in silica concentration are present even at long length scales, as shown by k-independent scattering at small k. The exact nature of the correlations present in the silica density fluctuations is described by the density-density correlation function $g(r)\equiv\langle\delta\phi(\vec{r})\delta\phi(0)\rangle$, where $\delta\phi(\vec{r})$ is the deviation of the local silica volume fraction from its average $\overline{\phi}$. For gels such as used here, $g(r)$ was determined experimentally, and is consistent with a correlation function [15]

$$g(r)=1.8\overline{\phi^2}e^{-r/\xi_G}/(r/\xi_G)^{3-D_f}. \quad (1)$$

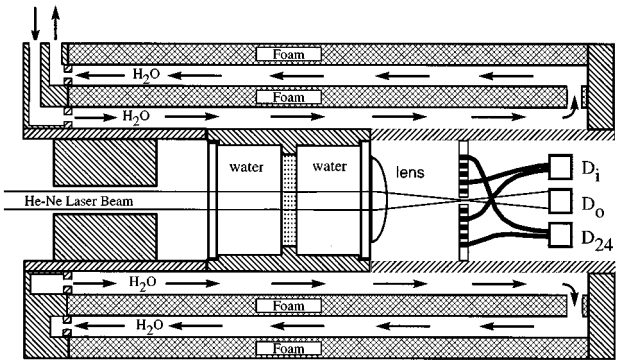

FIG. 1. Cross-sectional view of the cylindrical apparatus. The gel-mixture sample is contained in the dotted region. The arrows indicate the flow direction of the water used to control the sample temperature. The sample is bounded by 0.25-mm-thick flexible windows in the axial direction, and both the sample and the water in the adjacent chambers are pressure quenched together to minimize axial heat flow. The lens maps light scattered at a given angle onto a circle in a plane containing concentric rings of optical fibers leading to detectors D_1-D_{24}.

For the gels used in these studies, $D_f\simeq 2.2$ and $\xi_G\simeq 450$ Å.

To imbibe the mixtures into the gels, one window of each cell was removed, and IBAW mixtures of various concentrations were placed in contact with the gels. This procedure was carried out at 40 °C in the homogeneous phase of the IBAW mixture. The supernatant mixture, which had a volume of at least three times that of the gel, was replaced twice a day for four days. After equilibration the supernatant mixture was removed, and the cell window was replaced, ensuring that the average concentration of the mixture inside the gel could not change during the measurements. After the light-scattering studies were complete, the concentration of IBA in the gels was measured with an accuracy of ± 1 wt % by gas chromatography. The final concentrations of isobutyric acid in the fluid portions of the samples were 22-, 24-, 31-, and 35-wt % IBA.

B. Apparatus

The light-scattering apparatus used in these measurements was described previously [11], and is shown schematically in Fig. 1. The scattering cells described above were placed in the center section of the apparatus; the sample is shown as the dotted region in the center. The two chambers adjacent to the sample were filled with water. The pressure of the water and, thus, that of the sample was controlled by a feedback control system involving a solenoid activated piston, which could change the pressure by 250 psi in 15 ms. The sample pressure could be varied continuously from atmospheric pressure to 450 psi with a stability of ± 0.5 psi. Quenches were performed by suddenly lowering the pressure, which raised the sample's T_c and lowered the temperature of the sample and the water. The net effect was a $d(T-T_c)/dP\simeq 4.08$ mK/psi according to published values for $dT_c/dP=-55$ mK/atm [16] and $(dT/dP)_S=5$ mK/atm [12]. The sample temperature was controlled by a circulating water bath, as shown in Fig. 1, and was stable to ± 15 μK over 24 h.

Light scattered at an angle θ was mapped into a ring of diameter $f\tan\theta$ in the focal plane of a planoconvex lens of focal length $f=75$ mm. An array of 24 concentric rings composed of 0.5-mm-diameter optical fibers was placed in the focal plane and centered on the focused transmitted beam, which passed through a 1.0-mm-diameter hole in the center of the array and fell on a silicon photodiode D_0. Identical detectors D_1-D_{24} were used to measure the scattered optical power collected by each of the rings of fibers. The range of scattering angles was $0.72°\leqslant\theta\leqslant 12.8°$, corresponding to a range of scattering wave vectors $1722<k<30\,570$ cm^{-1}. Each ring had a spread in θ of $\Delta\theta\pm 0.25°$. The entire detector array could be sampled at a rate as great as once every 1.0 ms to determine the time-dependent scattering cross section $S(k,t)$. The scattered intensity was converted to absolute units using a previous calibration [11].

III. EXPERIMENTAL RESULTS

Stray light affected all of the lower-angle measurements, especially those made on low IBA concentration samples which scatter very weakly before the quenches. The amount of stray light was estimated and subtracted from the data by using the following facts: the structure factor of the system in the one-phase region is k independent at low k [8], and the stray light was a negligible fraction of the measured scattering at our largest k values. Typical stray light values were equivalent to a scattering cross section of 0.04 cm^{-1} at intermediate k, to as much as 4 cm^{-1} at low k, with an average value of 0.28 cm^{-1}.

Light-scattering measurements were made for each sample as a function of temperature, while the pure system's phase separation temperature was approached from 40 °C. Using the measured average concentration of the fluid portion of each sample together with the absolute scattered intensity, we were able to estimate [8] the concentration of the fluid not preferentially attracted to the gel, as shown in Fig. 2. Analysis of the scattered intensity is consistent with water being preferentially attracted by the silica; this fact is also consistent with the chromatography results. Note that the concentration of the nonadsorbed fluid in the 31- and 35-wt % IBA samples changes drastically near the critical point of the pure system as water is preferentially adsorbed.

The temperature T^* at which the three lowest-concentration samples entered the domain state was determined as follows. As the temperature was decreased in half-degree steps, both the intensity and the temperature of the sample were continuously monitored. For the three lower-concentration samples, the scattering increased discontinuously at all angles when the sample reached a particular temperature; we interpreted this temperature as T^*. After warming the sample approximately 0.2 °C above T^*, we confirmed T^* by making pressure quenches to effective temperatures approximately 0.1 °C above and below T^*. The results of the former showed a monotonic relaxation to a new scattering state, while the results of the latter showed definite overshoots in the scattered intensity. Values for T^* are shown as solid symbols in Fig. 2; the concentration of the nonadsorbed fluid for these points was estimated by extrapolating from data at higher temperatures [17].

We did not observe a discontinuous increase in the scattering of the highest concentration sample when reducing the temperature; every decrease in temperature resulted in a monotonic increase in the scattering. Consequently, we do *not* believe that this sample spontaneously enters the domain state upon cooling. However, by using rapid pressure quenching, we were able to locate an effective T^* value for this sample, analogous to the T^* values of the other samples. Rapid pressure quenches to below this temperature resulted in intensity overshoots, while similar quenches to higher values did not. The effective T^* value for this sample is also indicated in Fig. 2 as a solid diamond.

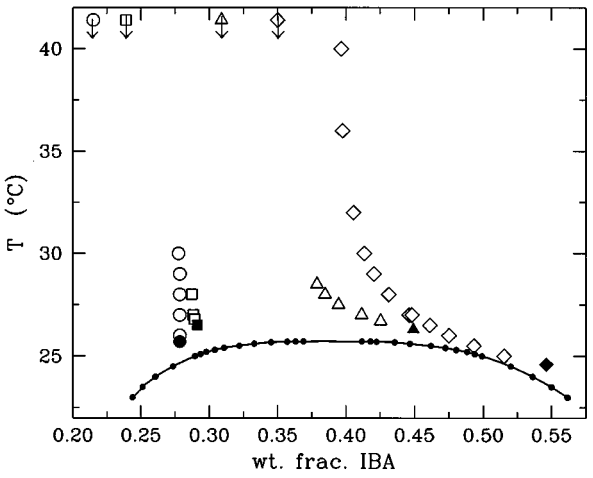

FIG. 2. Concentration of the nonadsorbed fluid as a function of temperature for each sample in the one-phase region. Coexistence curve data for the pure system [7] are shown as small solid circles. Large circles, squares, triangles, and diamonds correspond to samples with fluid portions containing 22-, 24-, 31-, and 35-wt % IBA mixtures, respectively. Large solid symbols show T^*. The symbols at the top of the graph indicate the average concentration of each sample as determined by gas chromatography.

The scattered intensity was measured as a function of time for pressure quenches to various distances below T^*. Results characteristic of the three lower-concentration samples are shown in Fig. 3. This figure shows the time dependence of the scattering for the 22-, 24-, and 31-wt % IBA samples following a pressure quench which effectively changed the temperature from 0.3, 0.2, and 0.3 °C above T^* to 0.4, 0.5, and 0.4 °C below T^*, respectively. The data show an increase in scattering of as much as six orders of magnitude relative to the prequench value (dashed line) during the first 1000 s following the quench. Because the laser power was reduced prior to the quench to accommodate the strong scattering late in the quench, data for early times, such as the 10-ms data of Figs. 3(a) and 3(b) are fairly noisy. Approximately 1.0 s after the quench, a peak in the intensity emerges at large k. As time progresses, the wave vector of the peak k_m decreases, and the amplitude of the peak $S(k_m)$ increases. By 1000 s the peak position has collapsed below our lowest k, and the intensity has started to decrease at all accessible k. Even before the peak appears at the largest accessible k, the scattering at very low k increases strongly, apparently independent of the peak formation and collapse.

Results characteristic of the highest-concentration sample are shown in Fig. 4. This figure follows the time dependence of the scattered intensity for the 35-wt % sample following a

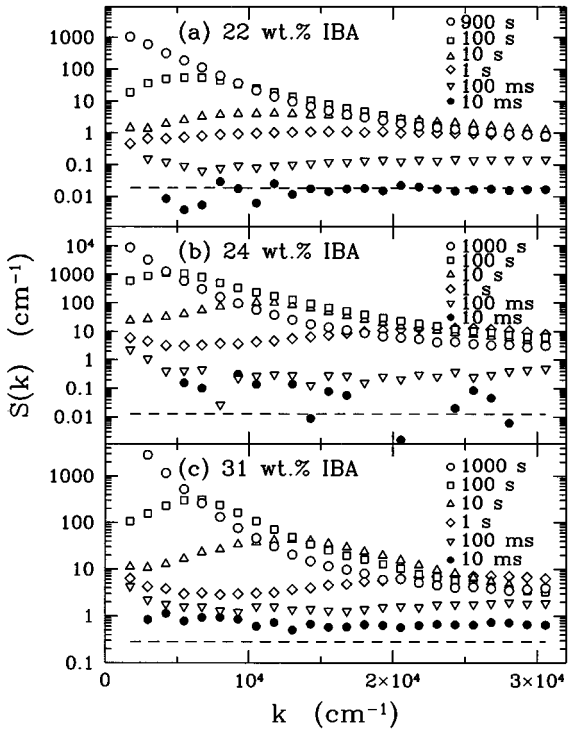

FIG. 3. Structure factor at various times following quenches to 0.4, 0.5, and 0.4 °C below T^* for the (a) 22-, (b) 24-, and (c) 31-wt % IBA samples respectively. The magnitude of the scattering from the samples before the quench was initiated is shown as dashed lines.

pressure quench from 0.5 °C above its effective T^* to 0.5 °C below. The behavior is similar to that of the low-concentration samples in some ways. One noticeable difference from the low-concentration samples is that the change in intensity during the quench is much smaller, only two orders of magnitude in this case. Furthermore, the sample relaxes more quickly than the low-concentration samples; by 1000 s, the scattered intensity has relaxed back to values observed just after the start of the quench.

Further examination of the data for individual k values reveals that the way in which the intensity increases following a quench is unusual. This behavior is shown in Fig. 5. During the early stages of the quench, the intensity increases virtually simultaneously at all accessible k. There is clearly

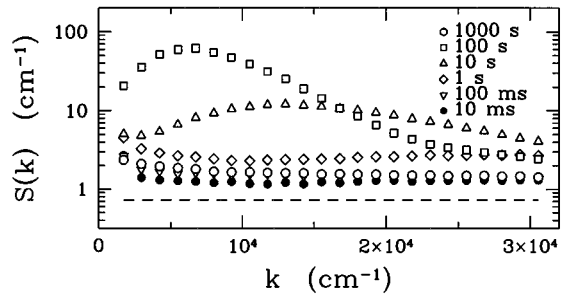

FIG. 4. Structure factor at various times following a quench to 0.5 °C below its effective T^* for the 35-wt % IBA sample. The magnitude of the scattering from the sample before the quench was initiated is shown as a dashed line.

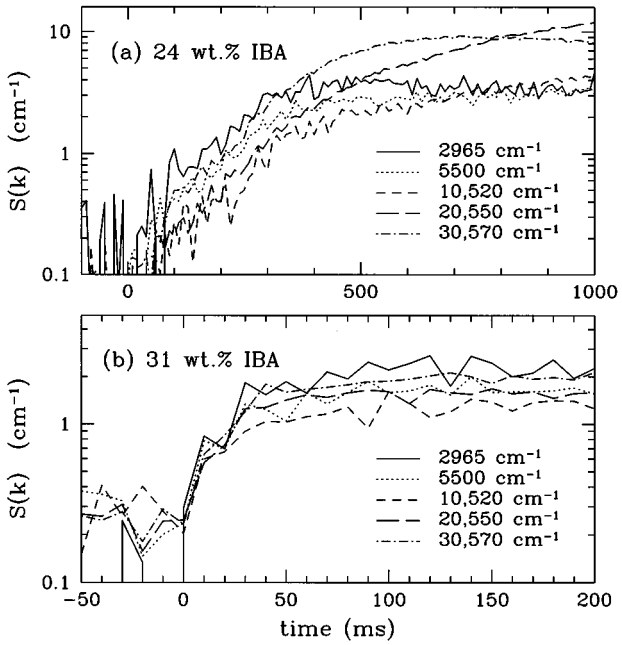

FIG. 5. Growth of scattered intensity as a function of time following the quench for selected wave vectors for (a) the quench shown in Fig. 3(b), and (b) the quench shown in Fig. 3(c). Note the difference in the time scales shown.

no strong k dependence of the growth rate, as would be the case for a diffusive process such as spinodal decomposition or nucleation in pure binary mixtures. In that case, the intensity at each k during the early stages of growth grows with a k-dependent growth rate determined by the diffusive time scale $(Dk^2)^{-1}$.

Furthermore, there are striking differences between how quickly the early increases in the intensity occur in low- and high-concentration samples. Figure 5 shows increases in intensity at several scattering wave vectors for the quenches shown in Figs. 3(b) and 3(c). For the sample which contains 24-wt % IBA, the scattered intensity initially shows a nearly exponential growth at a rate which is k independent. Subsequently, the data for $k = 20\,550$ continue to increase, and the data for $k = 30\,570$ cm^{-1} first increase and then decrease. These differences occur because the peak collapses through $k = 30\,570$ cm^{-1} at $\approx$700 ms and reaches $k = 20\,550$ cm^{-1} just beyond the time range shown. The intensity scattered by the 31-wt % IBA sample increases at a rate which is an order of magnitude faster than that of the lower-concentration samples, while the intensity scattered by the highest concentration sample was able to respond as fast as the control system could vary the pressure. Generally, this initial increase in the scattered intensity was nondiffusive, and appeared to stabilize before the peak in intensity moved in from high k.

We checked for various experimental explanations of this unusual behavior. The data shown in Figs. 3, 4, and 5 were corrected for turbidity by dividing by the transmitted beam power, converted to absolute units, and corrected for stray light. The raw (precorrected) data were checked to make certain this effect is not due to a sudden drop in transmitted intensity. The raw data continue to show an increase in intensity, while the transmitted intensity shows a decrease con-

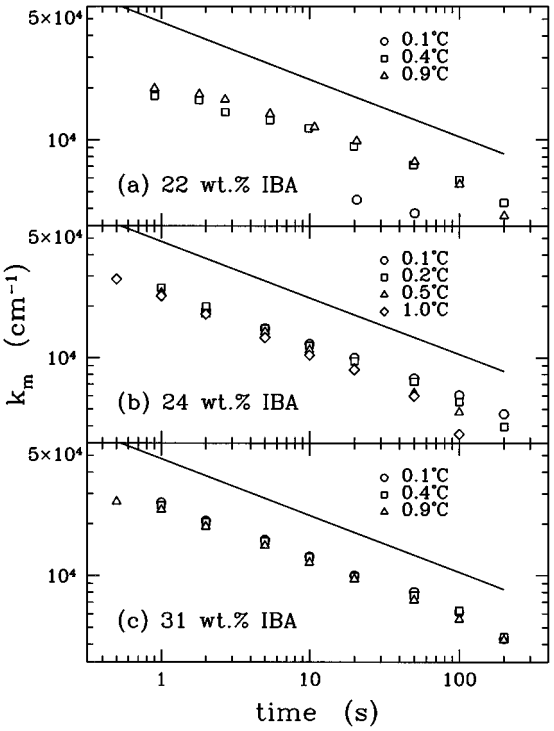

FIG. 6. Peak position k_m as a function of time for various quench depths below T^* for the (a) 22-, (b) 24-, and (c) 31-wt % IBA samples. The solid lines have a slope of $-\frac{1}{3}$ and a magnitude comparable to that measured in pure IBAW mixtures for off-critical quenches [12].

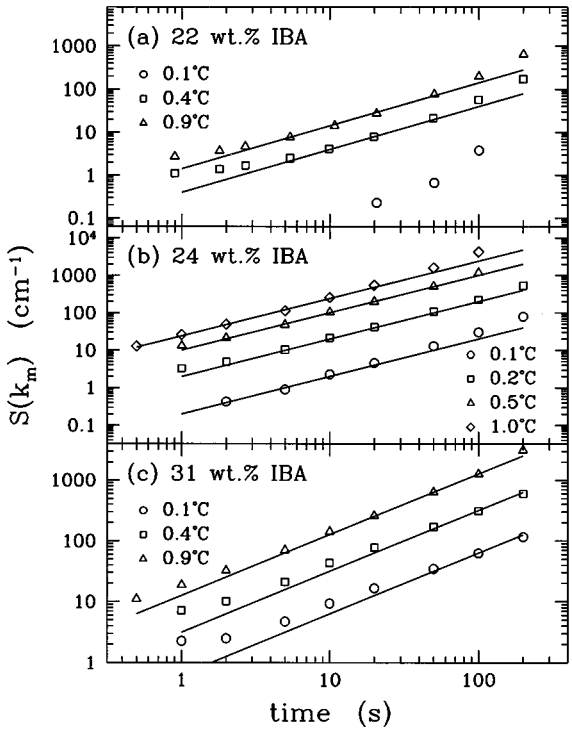

FIG. 7. Peak amplitude $S(k_m)$ as a function of time for various quench depths below T^* for the (a) 22-, (b) 24-, and (c) 31-wt % IBA samples. The solid lines have a slope of 1.0. Note that $S(k_m)$ evolves nearly linearly in time at all quench depths for these three samples.

sistent with the increased turbidity. We checked that the change in intensity is reversible and not due to an increase in the stray light of the system. We also performed simulations [18] to ensure that these observations are not due to multiple light scattering.

After a sample had remained in the quenched state for 1000 s, the pressure was increased to return the sample to prequench conditions. The samples appeared to reequilibrate to the prequench state within 15 min, but to obtain reproducible results they had to be left significantly longer between quenches. After all the desired quenches had been performed on a sample, it was cooled to a temperature 0.5 °C below T^*, and monitored for at least 12 h. After an initial increase in scattering, during which the samples became opaque, the scattered intensity decreased at all k, although more slowly in lower-concentration samples. The intensity scattered by the samples appeared to equilibrate to a structure factor comparable to that of the bare gel but with an amplitude larger than prequench values. The samples of this study cleared more quickly than those used in previous experiments, which were approximately 10 mm in diameter and 5 mm in height, and either took weeks to clear [8] or did not clear even within a period of weeks [7]. However, no meniscus indicating bulk phase separation was visible in the present samples even after they had cleared.

IV. ANALYSIS AND DISCUSSION

The location k_m and amplitude $S(k_m)$ of the peaks as functions of time were extracted from all data sets having well-defined peaks. Peaks were generally better defined for deeper quenches. Figure 6 shows the temporal evolution of k_m for the three lower-concentration samples for various quench depths. Except for the 0.1 °C quench of the 22-wt % sample, the evolution is consistent with $k_m \sim t^{-1/3}$. This, in itself, is somewhat surprising. Theoretical predictions for domain growth in the presence of quenched disorder [19] suggest a logarithmic time dependence due to pinning of the domain walls by impurities in the system. Instead, we found the same $t^{-1/3}$ dependence observed in pure mixtures for domains as large as we can measure with this technique, i.e., about 10 μm. This length scale is many orders of magnitude larger than the correlation length of the gel. Furthermore, the evolution of k_m is largely independent of the quench depth. In both of these ways, the data are consistent with the behavior observed in the pure mixture system during off-critical quenches [12]. However, the magnitude of k_m is approximately a factor of 2 smaller in the gel-mixture system than it is in the pure system; thus the length scale of the domains for the gel-mixture system is almost a factor of 2 larger at any given time than it is for the pure system. This is indicated by the solid lines in Fig. 6, which are representative of quenches G and H of Ref. [12], which correspond to samples containing about 34- and 32-wt % IBA, respectively. The fact that k_m as a function of time is essentially the same for all concentrations and all quench depths indicates that the factor of 2 difference is not due to prequench conditions.

Figure 7 shows the time dependence of $S(k_m)$ for the same quenches shown in Fig. 6. The lower-concentration samples (22-, 24-, and 31-wt % IBA) are generally consistent

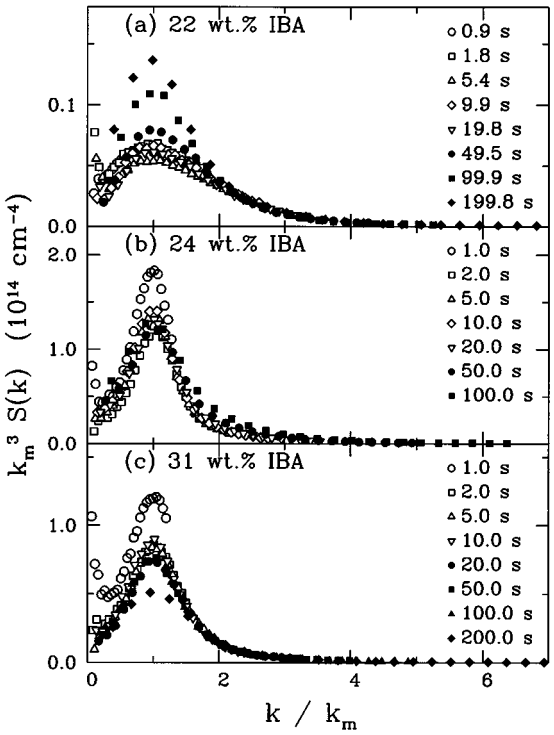

FIG. 8. Graphical test of the dynamic scaling hypothesis for the quenches shown in Fig. 3. Except for some deviations at early and late times, these samples appear to obey scaling.

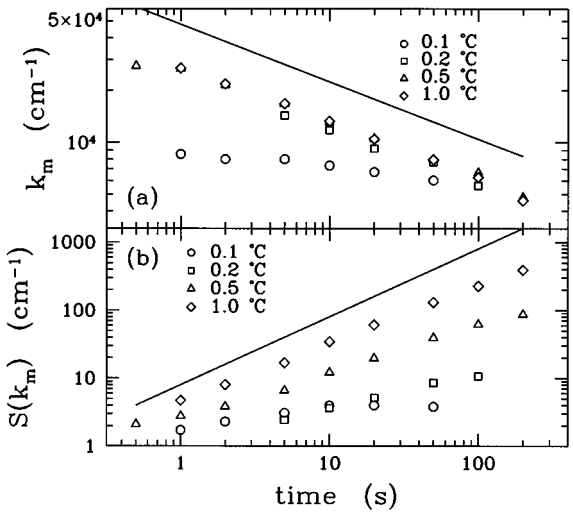

FIG. 9. (a) Peak position k_m as a function of time for various quench depths below the effective T^* for the 35-wt % IBA sample. The solid line has a slope of $-\frac{1}{3}$, and a magnitude comparable to that measured in pure IBAW mixtures for off-critical quenches [12]. (b) Peak amplitude $S(k_m)$ as a function of time for various quench depths below the effective T^* for the 35-wt % IBA sample. The solid line has a slope of 1.0. Note that $S(k_m)$ evolves in time with an exponent which depends on the quench depth.

with $S(k_m) \propto t$, as is observed for the pure system, although they show some deviation from this behavior at small and large t. The deviations at large t are the result of multiple scattering, as discussed below, and the deviations at small t are consistent with the peak being superimposed on the k-independent scattering that develops very quickly after the quench.

For the pure system, the existence of a single length scale k_m^{-1} characterizing the system dynamics leads to the dynamic scaling hypothesis [20] which predicts

$$S(k/k_m,t) = k_m^{-3}(t) F(k/k_m(t)), \tag{2}$$

where $F(x)$ is a universal scaling function. The result of plotting the data shown in Fig. 3 in the form $k_m^3\ S(k)$ as a function of k/k_m is shown in Fig. 8. Data for most quenches obey scaling fairly well, with significant deviations only at the earliest and latest times. Deviations from the scaling function at later times in the region beyond $k \simeq k_m$ are due to multiple scattering (see below); deviations at early times are consistent with the early onset of k-independent scattering.

Figure 9 shows the time dependence of k_m and $S(k_m)$ for quenches of various depths for the 35-wt % IBA sample. Behavior of k_m is similar to that seen in the lower-concentration samples except for the 0.1° quench. The behavior of $S(k_m)$ is not consistent with linear growth for any period of time following a quench. As a result, the data for the highest concentration sample, as shown in Fig. 10, did not scale over any significant period of time for any quench depth. In summary, the highest IBA concentration sample behaved quite differently from the other samples. The intensity $S(k_m)$ was more than an order of magnitude smaller than for the lower IBA concentration samples, it did not show linear growth with time, and this sample did not exhibit dynamic scaling. Recall that this sample shows no evidence of spontaneous domain formation on cooling, and that to find a temperature analogous to T^* for this sample we were forced to use pressure quenches; simply reducing the temperature led to a monotonic increase in the scattered intensity. We speculate that the dynamics of this sample are different from the others because the equilibrium state of the nonadsorbed mixture lies outside the coexistence curve of the pure mixture; this is consistent with the data shown in Fig. 2. The dynamics here may represent a competition between enhancement of the adsorbed layer, which tends to drive the nonadsorbed fluid away from the region of domain formation, and the process of domain formation. Such behavior can occur only in a system with a conserved order parameter, and should not be observed in dilute antiferromagnets.

Representative data were corrected for multiple scattering to determine the extent to which this phenomenon has af-

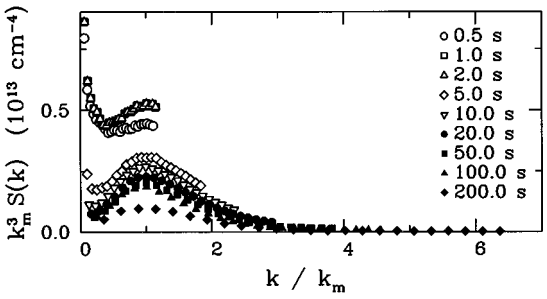

FIG. 10. Graphical test of the dynamic scaling hypothesis for the quench shown in Fig. 4. The 35-wt % IBA sample never obeys scaling.

fected our results. Corrections were performed using the algorithm prescribed by Bailey and Cannell [18]. The amount of multiply scattered light is simulated to all orders for a trial scattering cross section, which is then altered systematically until agreement with the data is obtained. The method, which was previously used to correct measurements of phase separation in a pure binary fluid mixture, nitroethane–3-methyl pentane, requires the use of a structure factor which is consistent with the data. The form used to fit the spinodal peak in the pure binary mixture data [18] is also consistent with the binary-mixture–gel data. These corrections show that the main effect of multiple scattering is to broaden the peak. There is negligible change in peak position, but there is a small ($\leqslant 15\%$) increase in the peak height due to contributions from odd orders of scattering. Deviation of $S(k_m)$ from a linear relationship with t at late times in the low-concentration samples is mainly attributable to this effect.

V. CONCLUSIONS

We have observed the growth and coarsening of domains which form spontaneously in the one-phase region of a gel-mixture system. The domains grow to length scales orders of magnitude larger than the correlation length of the gel structure (450 Å) without showing any evidence of pinning. The growth of the domains is characterized by the same $t^{1/3}$ dependence observed in pure mixtures when they are quenched into the two-phase region. For the three low IBAW concentration samples, which spontaneously formed domains on cooling, the scattering is consistent with the scaling hypothesis. However, unlike a pure binary fluid system, the intensity scattered by the samples increases simultaneously at all scattering wave vectors measured, even before the peak representative of domain growth has appeared. At long times, the gel-mixture system appears to remain in a domainlike state which we have not attempted to characterize.

Samples of the gel-mixture system which are sufficiently rich in water enter this domain state at temperatures comparable to the phase separation temperatures of the pure system. Previous measurements of critical fluctuations in this system [21] showed that the correlation length of the fluctuations grew as this region was approached, but only reached a size comparable to the correlation length of the gel before the transition to the domain state occurred. A thermodynamically stable two-phase region has been discovered at even lower temperatures [7].

In many ways this behavior is reminiscent of the behavior of doped antiferromagnets cooled in an applied field H. These systems are characterized by a disordered state at high temperature, and they fall out of equilibrium at a temperature $T_{\rm eq}(H)$ above the transition to the low temperature phase which does show long-range order [1]. However, the gel-mixture system appears to be able to reach equilibrium after falling into a domain state, whereas the field-cooled magnetic systems apparently remain in the domain state for extremely long times. Further work with the IBAW-gel system should help elucidate the nature of this new region of its phase diagram, and its relationship to the frozen-domain state of doped antiferromagnets.

ACKNOWLEDGMENTS

This research was supported by NSF Grant No. DMR 93-20726 and NSERC. The authors gratefully acknowledge helpful conversations with Profesor Joon Lee.

[1] See, for example, D. P. Belanger and A. P. Young, J. Magn. Magn. Mater. **100**, 272 (1991), and references therein.
[2] J. Villain, J. Phys. (France) **46**, 1843 (1985).
[3] J. V. Maher, W. I. Goldburg, D. W. Pohl, and M. Lanz, Phys. Rev. Lett. **53**, 60 (1984).
[4] F. Brochard and P. G. de Gennes, J. Phys. (France) Lett. **44**, L785 (1983); P. G. de Gennes, J. Phys. Chem. **88**, 6469 (1984).
[5] A. P. Y. Wong and M. H. W. Chan, Phys. Rev. Lett. **65**, 2567 (1990).
[6] A. P. Y. Wong, S. B. Kim, W. I. Goldburg, and M. H. W. Chan, Phys. Rev. Lett. **70**, 954 (1993).
[7] Z. Zhuang, A. G. Casielles, and D. S. Cannell, Phys. Rev. Lett. **77**, 2969 (1996).
[8] B. J. Frisken, F. Ferri, and D. S. Cannell, Phys. Rev. E **51**, 5922 (1995).
[9] A. J. Schwartz, J. S. Huang, and W. I. Goldburg, J. Chem. Phys. **62**, 1847 (1975).
[10] N.-C. Wong and C. M. Knobler, J. Chem. Phys. **66**, 4707 (1977).
[11] A. E. Bailey and D. S. Cannell, Phys. Rev. Lett. **70**, 2110 (1993).
[12] N.-C. Wong and C. M. Knobler, J. Chem. Phys. **69**, 725 (1978).
[13] J. C. Lee, Physica A **210**, 127 (1994).
[14] D. Avnir and V. R. Kaufman, J. Non-Cryst. Solids **92**, 180 (1987); B. Cabane, M. Dubois, F. Lefaucheux, and M. C. Robert, *ibid.* **119**, 121 (1990).
[15] F. Ferri, B. J. Frisken, and D. S. Cannell, Phys. Rev. Lett. **67**, 3626 (1991).
[16] G. Morrison and C. M. Knobler, J. Chem. Phys. **65**, 5507 (1976).
[17] We do not believe that the fact that T^* is generally *above* the coexistence curve of the pure system is significant. Previous work has shown that the location of T^* is very sensitive to impurities. A better sample-preparation method appears to involve pre-washing the gel with pure water before exposing it to the IBAW mixture [7].
[18] A. E. Bailey and D. S. Cannell, Phys. Rev. E **50**, 4853 (1994).
[19] J. Villain, Phys. Rev. Lett. **52**, 1543 (1984); G. Grinstein and J. F. Fernandez, Phys. Rev. B **29**, 6389 (1984); D. A. Huse and C. L. Henley, Phys. Rev. Lett. **54**, 2708 (1985).
[20] K. Binder and D. Stauffer, Phys. Rev. Lett. **33**, 1006 (1974); F. Furukawa, Physica A **123**, 497 (1984).
[21] B. J. Frisken and D. S. Cannell, Phys. Rev. Lett. **69**, 632 (1992).